



(RESEARCH ARTICLE)



Mass and topology optimization of tensegrity structures with application to footbridges

Lezin Seba Minsili ^{1,*}, Kankeu Mbefoyo King Jackson ², Okpwe Mbarga Richard Placide ³ and Baleng Blieriot Landry ⁴

¹ Associate Professor, Department of Civil Engineering, Yaoundé National Advanced School of Engineering ENSPY, The University of Yaoundé 1, P.O. Box 8390 Yaoundé, Cameroon.

² Ph.D. Student, Department of Civil Engineering, Yaoundé National Advanced School of Engineering ENSPY, The University of Yaoundé 1, P.O. Box 8390 Yaoundé, Cameroon.

³ Lecturer, Department of Civil Engineering, Yaoundé National Advanced School of Engineering ENSPY, The University of Yaoundé 1, P.O. Box 8390 Yaoundé, Cameroon.

⁴ Graduate Student, Department of Civil Engineering, Yaoundé National Advanced School of Engineering ENSPY, The University of Yaoundé 1, P.O. Box 8390 Yaoundé, Cameroon.

Publication history: Received on 25 August 2020; revised on 16 September 2020; accepted on 20 September 2020

Article DOI: <https://doi.org/10.30574/gjeta.2020.4.3.0064>

Abstract

This paper underlines the need of improving the traditional design method of stem rope footbridge by a sustainable reliable optimization design method of tensegrity footbridge. The proposed methodology displays the optimization of the topology of elements and of the structure, the specified loading and unloading procedures, and the system practical behaviour with respect to construction norms through the obtained multivariate objective function. Since tensegrity systems are characterized by geometric nonlinearity and larger displacements, a specific software program was developed using MATLAB build-in optimization codes. The developed combine mass and topology optimization procedure results in improved geometric and mechanical behaviour. Discussions are presently going on with involved local administration and with different national economical actors to financially foster the project feasibility.

Keywords: Optimization; Tensegrity; Topology; Footbridge; Prestress; Construction.

1. Introduction

A tensegrity system corresponds to an assembly of self-prestress elements (bars and cables) that are subjected only to axial loads. Prestressing introduces compressive efforts in bars and tensile efforts in cables, fixing the kinematic local degrees of freedom while conferring rigidity to the general system [1, 2]. This analysis results in a structure which can support external loads. As a consequence, all one-dimensional elements are capable of transmitting load in only one direction in the form of cables, springs or stiffened short columns. While benefiting from these interesting simple properties applicable to truss structures, tensegrity systems introduce a set of admissible criteria that yield to mechanisms with more complex topologies than for conventional structures and mechanisms [3, 4].

Over the last 60 years, Analysis on tensegrity structures was done in a descriptive manner at different stages with different experimental and geometrical techniques [5, 6, 7]. These analytical procedures proved the advantages of tensegrity structures over conventional ones: (1) all elements are only axially loaded, (2) a flexible specialization on the choice of material to bear only tensile or compressive stresses, (3) the simplification of element geometry, (4) the relatively small ratio of the mass of the system to the span to cover [8, 9]. The mass/span ratio factor is a very important

* Corresponding author: Lezin Seba Minsili

Associate Professor, Department of Civil Engineering, Yaoundé National Advanced School of Engineering ENSPY, The University of Yaoundé 1, P.O. Box 8390 Yaoundé, Cameroon.

factor to consider, as well the load carrying capacity, in bridge design and construction. A situation that is even acute in Africa with traditional and conventional design and construction methods that are yet to be converted to quasi-updated modern construction standards and regulations well understood and easy to implement by local design offices [10, 11].

The main objective of this work is to improve the traditional design and construction methods, used earlier to span rivers with difficult access, by a fast-understood methodology in the design of tensegrity systems. The proposed methodology underlines the optimization of the topology of the elements and of the system, the specific loading and unloading procedure, and the system practical analysis with respect to construction norms. Since tensegrity systems are characterized by geometric nonlinearity and larger displacement a specific software program was developed using MATLAB [12] build-in optimization codes taking into account the following elements' geometric and mechanical parameters: the initial configuration, the value of self-prestress, and the material property as shown in figure 1.c.

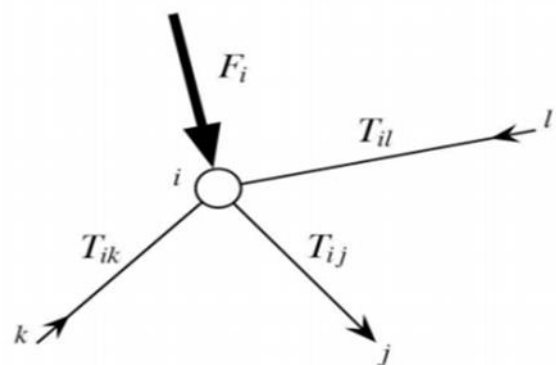
An application of the methodology is done on a local Government project to span the river banks of a rural less populated, but economically viable, area of the North West region of Cameroon. The structure of the footbridge is made up of a tensegrity framework system through which a wooden running surface, under a rectangular circulation gabarit, is reserved. This structure has a number of kinematics degrees of freedom and is also statically indeterminate, leaving the possibility of its elements to be prestressed. In order to reach expected results certain rules, pertaining to the quantity and length of cables, and to the running inner free space, are formulated to develop the optimized planar and spatial mechanisms forming the projected tensegrity footbridge. The developed combined mass and topology optimization procedure results in the reduction of the overall mass of the tensegrity footbridge as initial elements' section are specifically reduced from their initial value to their new optimized minimal one. Discussions are presently going on with the local administration of the construction site as well as with different national actors of the construction industry to financially foster the feasibility and the realization of this project.

2. Material and methods

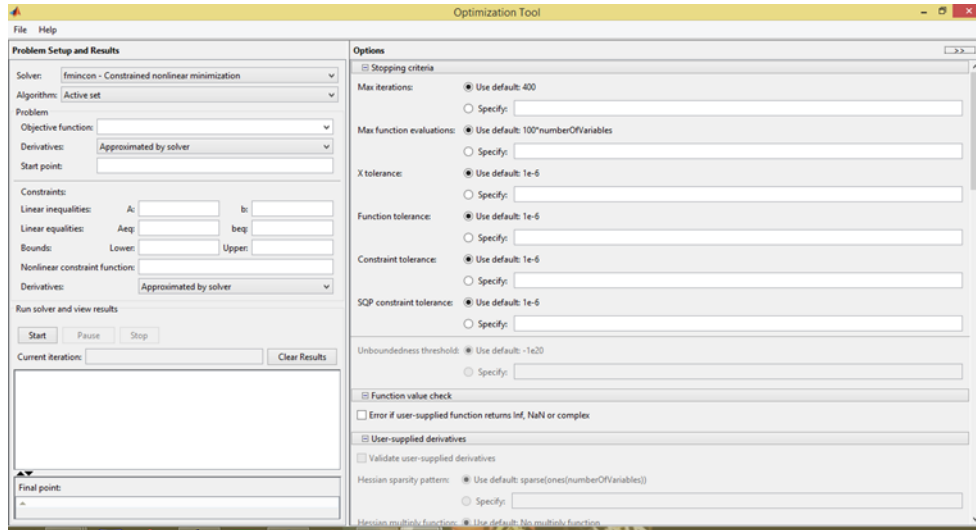
Elders in the Takamanda village of the South West of Cameroon are testifying that the knowledge to construct rope bridges with steams were common prior to the exploration and the westernization of the area [13]. The drawbacks of using mature stems of the small-diameter cane *Eremospatha Macrocarpa*, as the raw material for construction with a relatively short life span as observed in figures 1.a and 1.b, compel the society to turn to more reliable materials like steel and concrete with higher bearing capacity in comparison with these vegetal steams. For a more reliable material, the steam can be replaced by galvanized wire strands and the indigenous technology to construct the bridge itself can be improved with modern computational design. The design of tensegrity structures passes through three phases: the form finding phase or the determination of the geometry of the structure; the pre - stressing phase; and analyzing the structure under loading.



a) Existing rope bridge at Ollorunti river



b) Nodal forces equilibrium



c) MATLAB interface optimization tool

Figure 1 Local tensegrity systems in Cameroon with the proposed optimization tool.

2.1. Determination of the system geometry

Several analytical methods are used to find the optimal configuration of a tensegrid structure [14, 15], each displaying particular advantages and disadvantages depending on expected results. Two methods are used in this work: The Force Density Matrix method and the Dynamic Relaxation method. The force density matrix method [3] is used to deduce the internal stresses corresponding to a particular geometry under specific equilibrium conditions at each node. the equilibrium of the system is achieved when all nodes of the system are in equilibrium as shown in figure 1.b). Thus we have:

$$\sum_{j \neq i} T_{ij} + F_i = 0 \quad (1)$$

where: T_{ij} is the internal force j applied to node i ; F_i is the external force applied at node i .

Let x_i, y_i, z_i denote the spatial coordinates of node i and l_{ij}^0 the length of the element connecting nodes i and j , by projecting the above equation on the three axes, we obtain:

$$\begin{aligned} \sum_{j \neq i} T_{ij} \frac{x_j - x_i}{l_{ij}^0} + F_i^x &= 0 \\ \sum_{j \neq i} T_{ij} \frac{y_j - y_i}{l_{ij}^0} + F_i^y &= 0 \end{aligned} \quad (2)$$

$$\sum_{j \neq i} T_{ij} \frac{z_j - z_i}{l_{ij}^0} + F_i^z = 0$$

A system equation that can be simplified by introducing the force density of each element $q_{ij} = \frac{T_{ij}}{l_{ij}^0}$ to obtain the following equilibrium matrix equation at node i that can be solved by any nonlinear programming method :

$$\begin{aligned} \sum_{j \neq i} q_{ij} (x_j - x_i) + F_i^x &= 0 \\ \sum_{j \neq i} q_{ij} (y_j - y_i) + F_i^y &= 0 \\ \sum_{j \neq i} q_{ij} (z_j - z_i) + F_i^z &= 0 \end{aligned} \quad (3)$$

The dynamic relaxation method is based on the fact that any system under equilibrium with specified geometry and loading conditions, when elements constraints are imposed with appropriate intensities, generates unbalanced internal forces that produce the motion of the system prior to a new equilibrium position and a self-balanced configuration of

the system [16, 17]. Thus, from a given geometry and certain values of the internal forces imposed in the active elements, the nodal residues r is calculated, followed by the evaluation of the resulting velocities at the nodes and their new positions. the residuals are recalculated and the structure evolves accordingly until the final structure is obtained.

The position of the system can be determined by solving the dynamic equations. The dynamic relaxation method makes it possible to consider a structure without viscous damping and to calculate its successive motions until equilibrium is obtained. In the case of a cross-linked space system, the residual of unbalanced internal forces is evaluated at each node. For the node i in the direction x and at time t , we obtain:

$$R_t^{ix} = m_i \ddot{x}_t^i \quad (4)$$

The acceleration and the velocity at each time interval (t_{i-1}, t_i) are evaluated by the finite difference method. The convergence is ensured for the value of the mass m and the pitch Δt by the couple $m_i = \lambda k_i \Delta t^2$. For a given element with initial length L_u , uniform section A , a linear elasticity Young's modulus E , and at time t this element has a length L_t which corresponds to the normal internal solicitation:

$$T_t = EA(L_t - L_u)/L_u \quad (5)$$

The possibility of imposing a constant value on this effort ($T_t = cste$) is a major aspect that renders the concerned element to be active.

2.2. Design Principle of tensegrity systems

We address the problem of the design of tensegrity systems with the self-prestress principle leading to a set of geometric characteristics of undeformed cross sections of each element. In the case of flexible systems, the calculation is done in the context of geometric non-linearity with large displacements. The structural nonlinearity is viewed as material nonlinearity (associated with changes in material properties as well as in plasticity) [18] or as geometric (associated with configuration change, as is the case with slender elements in compression) one [19]. In this work the fundamental difference between a linear computation and a nonlinear geometric computation resides in the fact that the nonlinear computation is realized in a deformed configuration whereas the linear computation is carried out on an undeformed configuration [20, 21, 22]. This can significantly change the solution for systems undergoing significant displacements and the equilibrium equation of a loaded body is given as:

$$[K]\{u\} = \{f\} \quad (6)$$

where $[K]$ is the stiffness matrix ; $\{u\}$ is the displacement vector and $\{f\}$ is the vector of applied external force

For a non-linear calculation of tensegrity systems [23, 24], the stiffness matrix $[K]$ consists of three different terms namely the elastic rigidity term $[K_E]$, the non-linearity term reflecting the effect of large displacements $[K_{NL}]$, and the geometrical rigidity term considering the initial self-prestress $[K_G]$, and is given as:

$$[K] = [K_E] + [K_{NL}] + [K_G] \quad (6)$$

To evaluate the tangent stiffness matrix and the vector of the internal forces we get use of the Lagrangian formulation which leads us to:

$$\varepsilon_{GL} = \frac{L^2 - L_0^2}{2L_0^2} \quad (7a)$$

where L_0 and L are the length of the element in the initial and in the deformed configurations respectively.

If X_1, Y_1 and Z_1 are the element first node coordinates, and X_2, Y_2 and Z_2 its second node coordinates with $B_0 = \frac{1}{L_0} [-c_{0X} - c_{0Y} - c_{0Z} c_{0X} c_{0Y} c_{0Z}]$ and $H = \frac{1}{L_0^2} P = \frac{1}{L_0^2}$ then the previous equation becomes:

$$\varepsilon_{GL} = B_0 u + \frac{1}{2} u^T H u \quad (7b)$$

where: c_{0x} , c_{0y} and c_{0z} are the initial element cosine directions.

In the same manner the coefficient pertaining to the definition the deformed element, we can express the deformed configuration as $B = \frac{1}{L_0} [-c_x - c_y - c_z c_x c_y c_z] = B_0 + u^T H$. And for the determination of the tangent matrix and the internal forces, the first and the second order derivatives of the term ε_{GL} with respect to the displacement u is required. We thus have:

$$\frac{\partial \varepsilon_{GL}}{\partial u} = \frac{\partial (B_0 u + \frac{1}{2} u^T H u)}{\partial u} = B_0^T + H^T u = B_0^T + (u^T H)^T = (B_0 + u^T H)^T = B^T \quad (8)$$

$$H = \frac{\partial^2 \varepsilon_{GL}}{\partial u \partial u} = \frac{\partial}{\partial u} \frac{\partial \varepsilon_{GL}}{\partial u} = \frac{\partial B^T}{\partial u}$$

The stress corresponding to the Green Lagrangian deformation with the use of the initial Kirchhoff stress σ_0 constant over the element length with E as the Young's modulus is given as:

$$\sigma = \sigma_0 + E \varepsilon_{GL} \quad (9)$$

Differentiating the resulted stress component twice with respect to the displacement component u and making use of the theorem of potential energy we get expression of the internal stress p and the corresponding the tangent stiffness matrix $[K_T]$ deduced from it as:

$$p = \frac{\partial U}{\partial u} = V_0 \left(\frac{s_0 \partial e}{\partial u} + \frac{E e \partial e}{\partial u} \right) = V_0 (s_0 + E e) \frac{\partial e}{\partial u} = V_0 s \frac{\partial e}{\partial u} \quad (10a)$$

$$[K_T] = \frac{\partial p}{\partial u} = \frac{\partial}{\partial u} \left(\frac{V_0 s \partial e}{\partial u} \right) = V_0 E \frac{\partial e}{\partial u} \otimes \frac{\partial e}{\partial u} + V_0 s \frac{\partial^2 e}{\partial u \partial u} = K_M + K_G \quad (10b)$$

With \otimes being the Cartesian product between two vectors.

The expressions of these matrices are local matrices of each one-dimensional axial element whose matrices must be assembled into the global reference matrix. Knowing the expression of the tangent matrix and internal forces it is essential to look for an appropriate method to solve for nodal displacements since we can no longer determine the displacement vector by directly inverting the matrix $[K_T]$ because of the system nonlinearity. The Newton-Raphson iterative method [25] is used through the tangent stiffness matrix by reinitializing and reassembling the matrix $[K]$ at each iteration till we reach an equilibrium position P_1 with an applied load vector $\{\delta f^1\}$ and the next equilibrium is position P_2 under load the corresponding loading.

2.3. The regulatory framework

An effective design of tensegrity systems requires in advances the knowledge of the external conditions that the structure is subjected to, or in another hand we must define the limit states grouped in these two working conditions: the service limit states (SLS) and the ultimate limit states (ULS) according to the criteria given by the European construction norms EC3 [26].

At the SLS design all partial coefficients pertaining to the dead load (G) and to the live load (Q) are equal to unity, but for accidental loads their probability of occurrence limits the corresponding coefficient to 0.6 so as to consider the following load combination in the design:

$$G + Q + A + 0,6W \quad (11)$$

The design criteria of tensegrity systems in the SLS require the following verifications: the cable always remains tensile and the maximum deflection criterion is $1/200^{\text{th}}$ of its free span structure. At the ULS design, partial coefficients are different according to specified actions and initial pre-stressing. Since the self-prestress has a dual character in term of loading (an element is tensed up to a specified stress level) and of flexibility (an element rigidity is modified), loads combinations to be considered in design according to the European Standard EC3 are given for the favorable self-prestress case (0,8A) or for an unfavorable (1,2A) one as:

$$1,35 G + 1,5 Q + 1,2A + 0,6W \text{ (ULS 1)}$$

$$1,35 G + 1,5 Q + 0,8A + 0,6W \text{ (ULS 2)} \tag{12}$$

These verifications criteria of tensegrity systems in the ULS; permitting the cable relaxation under certain conditions are reduced to failure criteria under buckling of associated compressed bar elements and to tensile elastic limits of cables.

As we optimize the behavioral properties of a given structure in order to improve its functionalities under specific conditions, the structural optimization leads to the quality’s improvement in the design, construction and exploitation of infrastructures such as bridges, buildings or even space shuttles. This expected result requires that one looks at geometric and material characteristics of each element involved in the assembly of the structure as well as applied loading conditions. For civil engineering structures it is often common to balance the weight, the form and the robustness of structural components so as to find optimal values that best fit design requirements [27]. In the case of tensegrity systems, functional characteristics used during optimization are generally the weight (or the mass) and the element topology.

2.4. The Optimization of the Element’s Mass

The choice of variables related to the structural mass function toward an optimal decision making is crucial in order to minimize the objective function [28, 29]. In a one-dimensional bar element, the knowledge of the constraints and of the section and of a bar gives a straightforward description of the element mass provided that the latter is constant over its length.

Assuming that ρ_i is the material density of element I , of length L_i and section A_i , then system mass is given as $m = \rho \Sigma A_i L_i$ considering that the elements system has the same properties. And if the system is under equilibrium with known constraints thus the nodal equilibrium condition is given as $[A][q] = [f]$ where $[A]$ is the geometric matrix, $[q]$ is the element stress vector and $[f]$ is the external loads vector. Defining allowable stress variables of cables (with subscript c) and of bars (with subscript b) as the stress (q_c, q_b), the section (A_c, A_b) and the allowable stress in the elements (σ_c, σ_b), σ_y being the yielding rupture stress and ϵ_k the element deformation between the initial length L_0 and the final length L_k of the element, then the displacements constraints of the bars and the cables are defined respectively as:

$$-\frac{A_b \sigma_k}{l_b} \leq q_b \leq \frac{A_b \sigma_k}{l_b} \Rightarrow \begin{cases} q_b - \frac{A_b \sigma_k}{l_b} \leq 0 \\ -q_b - \frac{A_b \sigma_k}{l_b} \leq 0 \end{cases} \tag{13a}$$

$$0 \leq q_c \leq \frac{A_c \sigma_k}{l_c} \Rightarrow \begin{cases} q_c - \frac{A_c \sigma_k}{l_c} \leq 0 \\ -q_c \leq 0 \end{cases} \tag{13b}$$

Suppose our structure has b bar-elements with above defined constraints we define a vector x of order $2b$ described as $x_i = A_i$ for $i \leq b$ and $x_i = q_{i-b}$ for $b < i \leq 2b$ while applying the change of variables for each element e the mass optimization problem for a tensegrity system can have the following formulation that can be solve easily using the commercial MATLAB software [12]:

$$\begin{cases} \text{Find :} & x_i, i = 1, 2, \dots, 2b \\ \text{min :} & m = CX \\ \text{s. t. :} & AX \leq B \\ & A_{eq} X = B_{eq} \\ & X \geq L_B \end{cases} \tag{14}$$

2.5. The Topology Optimization

The topology of tensegrity system structures is characterized by the geometry and the connectivity between nodes through structural elements with indications on its mechanical state providing a bar or a cable functionality. The optimization procedure here is to minimize the number of cables used in the structure with an appropriate nodal position via an integral programming [30, 31]. Considering a structure having b elements (cables or bars exclusively) and n nodes, and initial self-stress q_i in equilibrium, then the following study domain $E = S U C U N$, made of corresponding subdomains and related positions (x_i, y_i) , is characterized by:

$$\begin{cases} q_i < 0 \text{ if } i \in S \text{ for a bar} \\ q_i > 0 \text{ if } i \in C \text{ for a cable} \\ q_i = 0 \text{ if } i \in N \text{ if an element is removed} \end{cases}$$

$$\begin{cases} (x_i, y_i) = (1, 0) \Leftrightarrow i \in S \\ (x_i, y_i) = (0, 1) \Leftrightarrow i \in C \\ (x_i, y_i) = (0, 0) \Leftrightarrow i \in N \end{cases} \quad (15)$$

Using two additional constants M and ε , infinitely great and infinitely small respectively, such that $0 < \varepsilon \ll M$, and the function $a_i(\xi_s, \xi_c)$ where ξ_s and ξ_c are positives constants, we introduce the value $a_i = \xi_s x_i + \xi_c y_i$ in equations 15 after transformations and reorganization to get a better expression of the initial self-stress:

$$\begin{cases} -\bar{q}_s \leq q_i \leq -\underline{q}_s \text{ if } i \in S \\ \underline{q}_c \leq q_i \leq \bar{q}_c \text{ if } i \in C \\ q_i = 0 \text{ if } i \in N \end{cases} \quad (16)$$

with $\bar{q}_s, \underline{q}_s, \bar{q}_c, \underline{q}_c$ being positive constants characterizing the upper and the lower bound of the stress in the element.

To define constraints on internal stress in each element we consider the nodal displacement u , and we write the deformation on the element by the expression $c_i = h_i^T u \quad \forall i \in E$, where $h_i \in \mathbb{R}^b$, each stress s_i in element being compatible with deformation c_i and expressed as:

$$s_i = \begin{cases} k_{si} c_i & \text{if } i \in S \\ \max(k_{ci} c_i, 0) & \text{if } i \in C \\ 0 & \text{if } i \in N \end{cases} \quad (17)$$

where k_{si} and k_{ci} are also positive constants defined as $k_{si} = E \xi_s / l_i$ and $k_{ci} = E \xi_c / l_i$, E being the usual Young modulus. We can write

$$\begin{cases} s_i = k_{si} c_{si} + k_{ci} c_{ci} \\ M x_i \geq |c_{si}| \\ M(1 - x_i) \geq |c_{si} - h_i^T u| \\ M y_i \geq |c_{ci}| \\ -M(1 - y_i) \leq c_{ci} - h_i^T u \leq M(1 - y_i) + M(1 - z_i) \\ -M x_i \leq s_i \leq M z_i \\ z_i \in \{0, 1\} \end{cases} \quad (18)$$

We partition the above domain as $J_N \cup J_D = \{1 \dots d\}$, where J_N is the subdomain of nodes on which external forces are applied, and J_D is the subdomain of nodes with zero displacement, in order to relate equilibrium conditions with initial self-stresses on a given element [28, 32]. Defining the variable $\tilde{s}_i = s_i + q_i$, we also introduce a new allowable stress-value \tilde{s}_i that can be transformed using lower and upper bound allowable stresses $\tilde{s}_s^{lb}, \tilde{s}_s^{ub}$ et \tilde{s}_c^{ub} verifying the conditions $\tilde{s}_s^{lb} > 0, \tilde{s}_s^{ub} \geq \bar{q}_c$ et $\tilde{s}_c^{ub} > 0$, in order to get the following expression:

$$\begin{cases} (-\tilde{s}_s^{lb} + \underline{q}_s) x_i \leq k_{si} c_{si} \leq (\tilde{s}_s^{ub} + \bar{q}_s) x_i \\ -\bar{q}_c y_i \leq k_{ci} c_{ci} \leq (\tilde{s}_c^{ub} - \underline{q}_c) y_i \end{cases} \quad (19)$$

External forces applied at nodal points f_j are also modelled through the equilibrium equation obtained from the maximum allowable work \bar{w} done by all external forces that structure can withstand without any failure, and we thus obtain:

$$w = \sum_{j \in J_N} f_j u_j \leq \bar{w} \quad (20a)$$

$$(Hs)_j = f_j, \quad j \in J_N \quad (20b)$$

From now on we can formulate the objective function of our topology optimization reduced to the minimization of the number of cables $|C| = \sum_{i=1}^m y_i$, while maintaining the mass optimization of the previous section, as given in the following optimization system equation that can also be solved using the commercial MATLAB software :

$$\left\{ \begin{array}{ll} \text{Find :} & x_i, y_i, z_i \quad i = 1, 2, \dots, 2b \\ \text{min :} & |C| = \sum_{i=1}^m y_i \\ \text{s. t. :} & Hq = 0 \\ & -\bar{q}_s x_i \leq q_i \leq (\underline{q}_s + \underline{q}_c)(1 - x_i) - \underline{q}_s \quad \forall i \\ & -(\bar{q}_s + \underline{q}_c)(1 - y_i) + \underline{q}_c \leq q_i \leq \bar{q}_c y_i \quad \forall i \\ & \sum_{i \in E(n_j)} x_i \leq 1 \quad \forall n_j \in V \\ & f^T u \leq \bar{w} \\ (Hs)_j &= f_j, \quad \forall j \in J_N \\ u_j &= 0 \quad \forall j \in J_D \\ s_i &= k_{si} c_{si} + k_{ci} c_{ci} \quad \forall i \\ (-\bar{s}_s^{lb} + \underline{q}_s) x_i &\leq k_{si} c_{si} \leq (\bar{s}_s^{ub} + \bar{q}_s) x_i \quad \forall i \\ M(1 - x_i) &\geq |c_{si} - h_i^T u| \quad \forall i \\ -\bar{q}_c y_i &\leq k_{ci} c_{ci} \leq (\bar{s}_c^{ub} - \underline{q}_c) y_i \quad \forall i \\ -M(1 - y_i) &\leq c_{ci} - h_i^T u \leq M(1 - y_i) + M(1 - z_i) \quad \forall i \\ -\bar{s}_s^{lb} &\leq q_i + k_{si} c_{si} \leq \bar{s}_s^{ub} \quad \forall i \\ -\bar{q}_s x_i &\leq q_i + k_{ci} c_{ci} \leq \bar{s}_c^{ub} \quad \forall i \\ x_i &\in \{0,1\}, \quad y_i \in \{0,1\}, \quad z_i \in \{0,1\} \quad \forall i \end{array} \right. \quad (21)$$

3. Results

3.1. Material Properties

The optimization methodology developed in this work is applied on the design of a simplified pedestrian classical tensegrity cable footbridge to cross the Ollorunti river portrayed in figures 1.a and 1.b, formally and actually crossed by traditionally made steams cable bridges. After a technical survey on site by our team a proposition to design a cable tensegrity bridge with cables and bars available on the local construction industry taking into account the needs of farmers to carry their products on tricycles from their farms to the local market through a rectangular circulation gabarit of 2.5m high and 1.75m wide as pictured in figures 2.a and b. The construction of a concrete was not appropriate due to financial technical constraints as well as the need of a middle concrete pier construction right on the river mainstream and a tensegrity bridge of 120.0m span from the two riverbanks of the selected appropriate location.

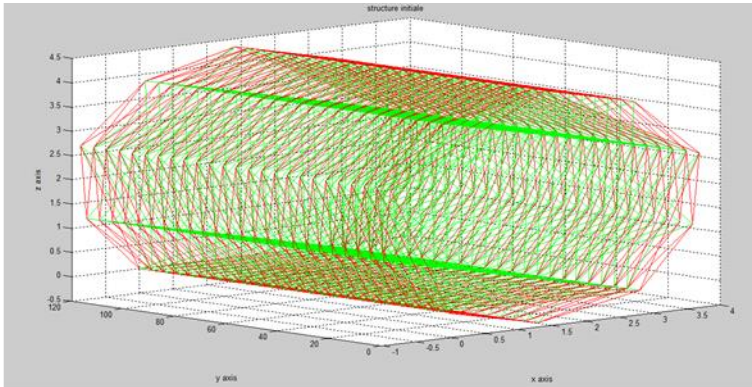
The basic geometry of a tensegrity ring, carrying the circulation running platform with the circulation free space, is that of a right prism whose generating polygon is either a square, a pentagon, or a hexagon. A study conducted on these three generating polygons [33, 34, 35] for the design of pedestrian footbridge has shown that the pentagonal-based module is the most stable one. The pentagon-based module, shown in figure 2.b), is therefore used in our application to obtain a combination of different modules in the form of a tensegrity framework shown in figure 2.a).

Given the fact that we have a multi-modular structure, the coordinates of each node of the module as well as the elements connectivity are appropriately chosen in order to easily generate, from required shape functions, the system local and global coordinates. The module, visualized in figure 2.c) and 2.d), and the system geometries providing the circulation gabarit of 1.75m×2.4m are also generated by specific formulae linking the corresponding coordinates of the nodes with the required space.

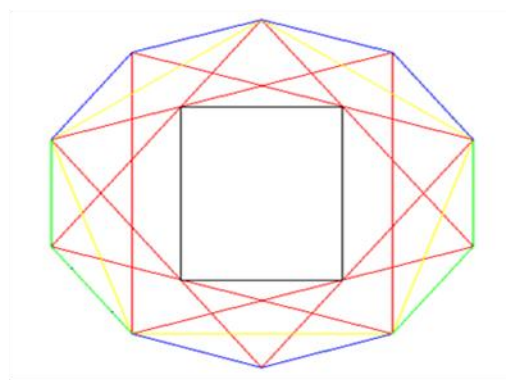
Considering that an elementary module has seven self-prestress states and mechanisms we assemble a multi-modular structure with node and element numbers generated from the expressions described below. Let n_m be the number of nodes in a module spanning 5.0m, with the span of the structure $L=120.0m$, and m the number of modules, two modules being interconnected by 5 nodes at their direct interface, then the total number of nodes in the structure is $N = n_m + (n_m - 5) \times m = 245$. The number of elements in our structure is $n_{el} = 45 + 40 \times (n_m - 1) = 965$, one element having 45 elements. A

detailed FEM programmed in MATLAB, with the MATLAB simplified code proposed as indicative in appendix, reveals that we have seven self-prestress states and six mechanisms for an elementary module.

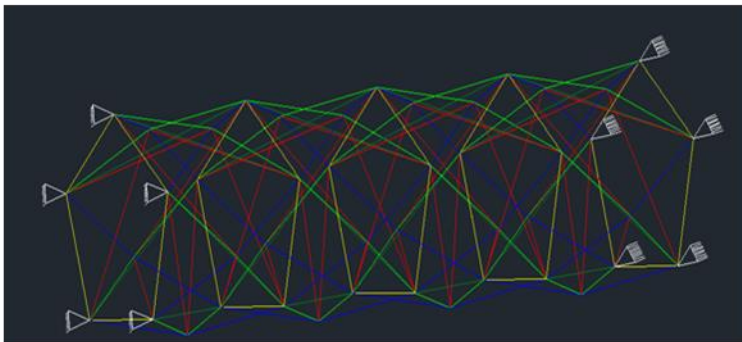
As was stated earlier, the three main properties contributing to an optimal choice of the materials (or the type of element i.e. bar or cable) are the mechanical properties, the stress /self-weight ratio, and the cost. These characteristics of the bars and cables are summarized below: the initial section of the cables is $S_c = 22 \text{ cm}^2$, and of the bars is $S_b = 75 \text{ cm}^2$; the Young's modulus of the cables is 125 GPa, and for bars is 200 GPa; and the admissible stress limit for the bars is 235 MPa, and for cables is 500 MPa. An expected optimal principle during the methodology in this work is that, under loading, the admissible limit stresses of bars and cables are required to be achieved in the same instant. The decking slab under the running surface is made of Group 2 wood materials, namely Bubinga (*Guibourtia tessmannii*) [36], well treated in order to resist outside effects such as moisture, temperature variation and insects' attacks.



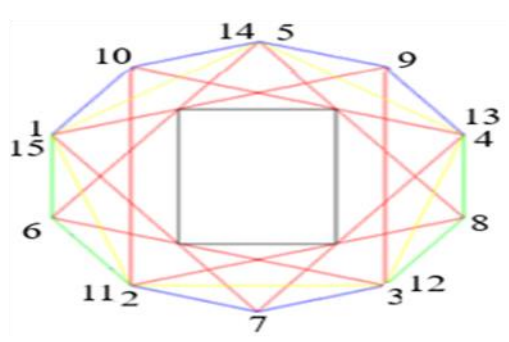
a) 3D image of the tensegrity framework (green=bars, red =cables)



b) Module front projection



c) Boundary end-conditions of a 2-module structure



d) Module nodes visualization

Lateral █ and intermediate █ bars; Nape █, coplanar █ and non-coplanar █ cables.

Figure 2 Analytical model of the tensegrity structure under study.

Ron Dennis [37] proposed to adopt for community infrastructures at rural and district levels a uniform distributed lively load of 400 kN/m^2 . Assuming that an average weight of an adult is 70 kg carrying an over load of 30 kg from the farm we roughly adopt, taking into consideration local environment in the community, that we will have a maximum number of 80 persons on the bridge at an unrealized peak period. This gives us the first loading case $Q_{L1} = 52 \text{ Kg/m}^2$ (0.52 kN/m^2). The second loading case Q_{L2} is taken as a loaded tricycle at the bridge midspan having a gross weight of 1000 kg (10.0 kN). For each of these loading cases we verify the maximum deflection limit ($L/200$, [37]) related to the elements' absolute tensile criteria in service limit state (SLS), and the allowable elastic stress ($\sigma_{lim} = A_c \times f_y$) of elements in the ultimate limit state (ULS_i), considering that their local and general stabilities criteria and those of the tensegrity system are verified.

3.2. Discussion

The proposed optimization procedure has produced, using the developed interface programming software based on the FEM. The deflection curves, pictured in figures 3 for the two loading cases in SLS, shows that obtained deflections of the designed tensegrity footbridge are below the maximum allowable value $L/200 = 120/200 = 0.60 \text{ m}$. The loading case 1,

representing an extremal unexpected case of eighty (80) villagers loaded with farm products comfortably walking on the bridge in the same momentum, has a maximum deflection of 0.467 m with high structural safety.

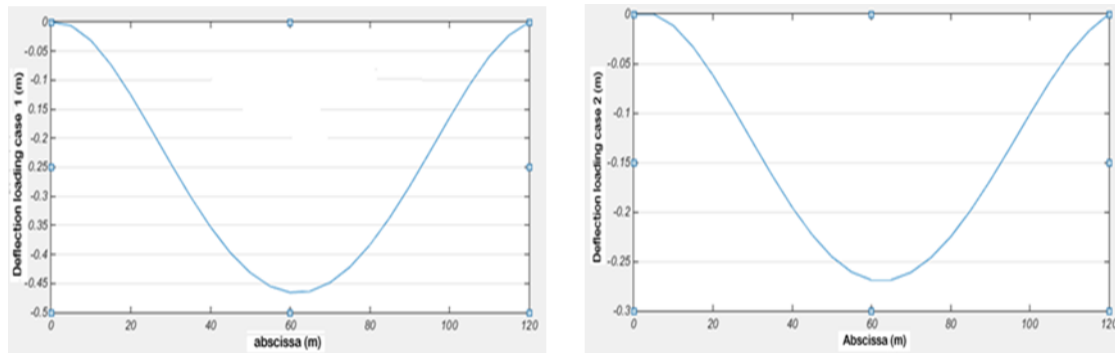


Figure 3 Deflection of the tensegrity structure for SLS loading cases 1 and 2.

A detailed observation made during the optimization process reveals that, for each loading case of every ULS, internal forces in bars and cables remains below the corresponding allowable value as it is depicted in figures 4 below. These results also justify why it is recommendable to replace tensile bars with cables, the later displaying a great margin of security before failure and a high level of cost reduction due also to volume of material reduction, each specific element in its own reduction rate, in tension or in compression.

The present optimization procedure reaches stable results after several iterations as any infinite small change, in section or/and in stress of a particular element, produces a noticeable reverse effect on the overall structural configuration and elements mechanical behaviour. This fact is the primary justification of the adopted mass-topology optimization optimality, during which all tensile bars are replaced by cables, and the self-prestress process in a cable is changed too to an optimal value that may lead to its release or to its strengthening. Since the adopted iterative procedure does not allow to observe the bifurcation point bypassing it searching for an adequate stable optimum, the number of released/strengthened cables is quite important: 312 and 316 for loading case 1 (C1) in ULS1 and ULS2 respectively, while the loading case 2 (C2) reaches 302 and 307 in ULS1 and ULS2 respectively. This number of iterations and relaxations leading to obtained results using the present methodology, would have not been made with an ordinary traditional structural design method.

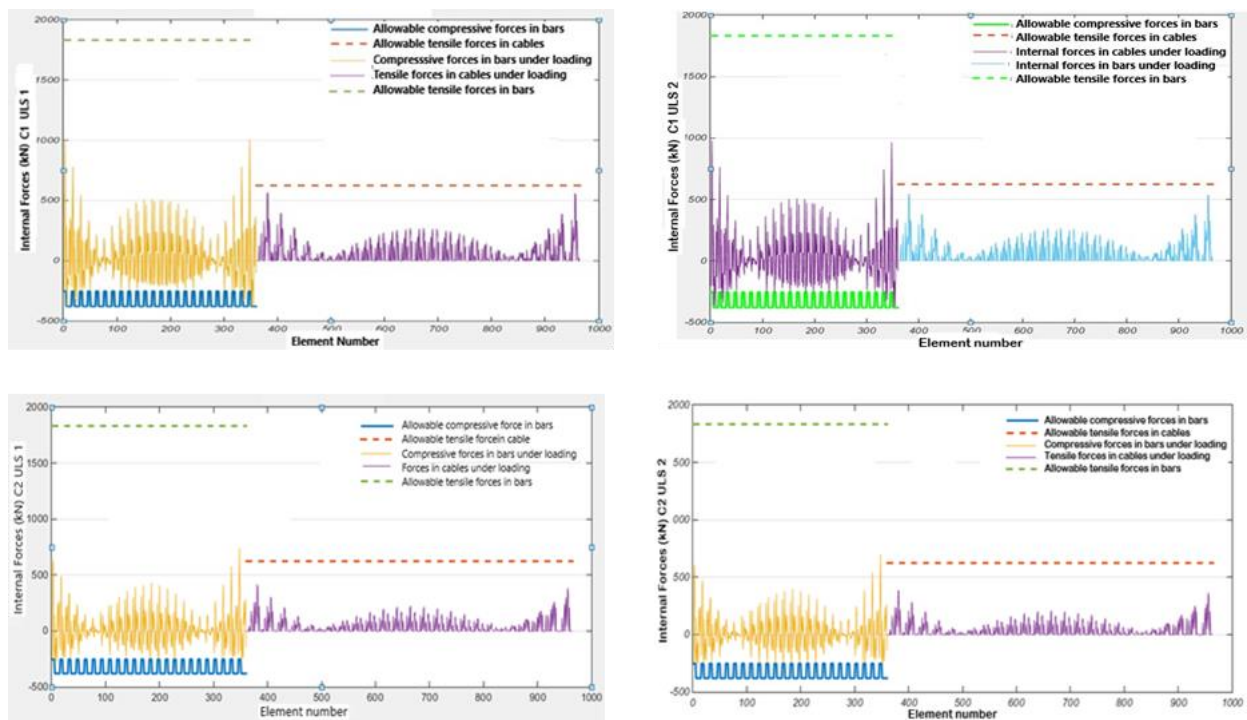


Figure 4 Internal forces for loading cases 1 (C1) and 2 (C2) in ULS;

The optimization procedure, resulting in the reduction of the overall mass of the tensegrity bridge, shows in figure 5 how the initial section of each element has been specifically reduced from its initial value to its new optimized one, with the application done only for the second loading case in ULS2. For the practical implementation of obtained results on site, a special care must be given to reduce the number of elements types out the 965 elements' sections. A probabilistic analysis is required, with available sections of bars and cables in the local construction industry, to define the number of sections representative on a particular interval range.

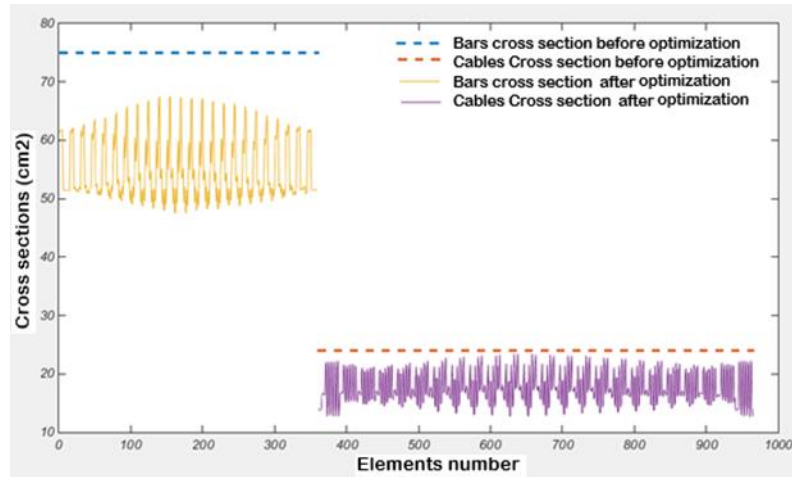


Figure 5 Cross sections' elements before and after optimization.

The optimization procedure, resulting in the reduction of the overall mass of the tensegrity bridge, shows in figure 5 how the initial section of each element has been specifically reduced from its initial value to its new optimized one, with the application done only for the second loading case in ULS2. For the practical implementation of obtained results on site, a special care must be given to reduce the number of elements types out the 965 elements' sections. A probabilistic analysis is required, with available sections of bars and cables in the local construction industry, to define the number of section's representatives on a particular interval range.

4. Conclusion

The optimization design of tensegrity footbridges is proposed in this paper with an application done on an existing traditionally build stems rope bridge to be replaced by an optimized tensegrity steel footbridge of 120 m span in Ollorunti county in the North West Region of Cameroon. The proposed methodology takes into account into three distinct related steps: the initial configuration of the structure leading the definition of initial geometric and initial properties, the optimization of the topology and the sections of individual elements with respect to existing design and construction standards, and level of self-prestress and relaxation applied to the and cables without he lost of stability.

Achieving the stability requirements on both the shape, the geometry and the material strength of each element, an optimal solution requires a simultaneous resolution the given optimization problem involving the topology and the self-prestress problem with an adequate release/strengthening of elements. A comprehensive MATLAB based program using the theory developed in this work allowed us to optimize output results in term of geometric properties, mechanical properties and stability conditions through the proposed well defined multivariate objective function. The objective function in this work minimizes the overall weight as a functional of several interdependent variables subjected to well defined geometric, mechanical and stability criteria.

Obtained results are showing that tensegrity footbridges are very sensitive to the change of initial conditions, and therefore more flexible, but allows to span larger distance with minimal required volume of material or construction costs. Consequently, the developed design tool has motivated the county local authorities to cooperate with the authors of this work in order to further the feasibility studies, the financing and the construction phases of the project, to implement the present findings and to ease the work of the design office involved with the Ollorunti county footbridge.

Compliance with ethical standards

Acknowledgments

The present work was done in the *Mechanical and Civil Engineering Laboratory (LECM)* of the National Advanced school of Engineering (ENSPY) of the University of Yaoundé 1, under the supervision of Professor Louis Max Ayina Ohandja to whom goes our great recognition.

Disclosure of conflict of interest

The author(s) declared no potential conflicts of interest with respect to the research, authorship and publication of this article.

Author's contributions

Lezin Seba Minsili initiated the project, suggested the methodology to be used, and oversaw the overall research work in relation with actors of the local construction industry; Kankeu Mbefoyo King Jackson proposed the structural mechanics and optimization theory developed in this work; Okpwe Mbarga Richard and Baleng Bleriot implemented the MATLAB code and the appropriate numerical interface. All authors discussed the results, reviewed and approved the final version of the manuscript.

References

- [1] Ángel Otoniel González Martínez et al. Dynamical Behavior of a Tensegrity Structure Coupled to a Spatial Steel Grid. *Current Journal of Applied Science and Technology*. 2019; 38, Issue 2: 1-24.
- [2] Luis Miguel Posada. Stability Analysis of Two dimensional Truss Structures. Master Degree Thesis, University of Stuttgart, Germany. 2007; 88.
- [3] Bel Hadj Ali N, Rhode-Barbarigos L, Pascual Albi A, Smith I.F.C. Design optimization and dynamic analysis of a tensegrity-based footbridge *Engineering Structures*. 2010; 32 (11): 3650-9.
- [4] Ankit kumar, Prasiddhi Mehta, Kamlesh Mandloi, Shashank verma, Rajat Patel, Avinash singh. Review Paper of Tensegrity Structure, *International Research Journal of Engineering and Technology (IRJET)*. Nov 2018; 05(11): 997-1000.
- [5] Andrea Micheletti. modular tensegrity structures: the torvergata footbridge. *Mechanics, Models and Methods in Civil Engineering*. 2012; 375-384. Dipartimento di ingegneria civile, Università di Roma Torvergata, via politecnico 1, 0013, Roma, Italy.
- [6] ANGELLIER Nicolas. Etat d'autocontrainte des grilles de tenségrité vers l'identification sous sollicitation naturelle. Thèse de doctorat à l'université de Montpellier II, France. 2008; 156.
- [7] Yoshihiro Kanno. Topology optimization of Tensegrity Structures via Mixed Integer Programming. 9th World Congress on Structural and Multidisciplinary Optimization. June 13-17, 2010.
- [8] Milenko Masic, RE Skelton, PE. Gill. Optimization of tensegrity structures. *International Journal of Solids and Structures*. 2006; 43: 4687-4703.
- [9] Skeleton RE, F Fraternali, G Carpentieri, A Micheletti. Minimum mass design of tensegrity bridges with parametric architecture and multiscale complexity. *Mechanics Research Communications*. 2014; 58: 124-132.
- [10] Plescan Costel Mircea Conțiu Adam Dosa. A study of a tensegrity structure for a footbridge. 3rd China-Romania Science and Technology Seminar. 2018.
- [11] IOP Conference Series: Materials Science and Engineering. 6.
- [12] Gerardo Carpentieri, Robert E Skelton, Fernando Fraternali. Minimum Mass and Optimal Complexity of Planar Tensegrity Bridges. *International Journal of Space Structures*. 2015; 30 (30 & 40): 221-243.
- [13] Optimization Toolbox™, User's Guide. The MathWorks, Inc., 3 Apple Hill Drive, Natick, MA 01760-2098. COPYRIGHT: 1990-2008 by. The MathWorks, In Technical Support. 2008; 575.
- [14] Sunderland Terry CH, Michael Balinga PB, Jacqueline L Groves. The cane bridges of the Takamanda region, Cameroon. *PALMS*. 2002; 46(2).

- [15] Salah Drabla, Ziloukha Zellagui. Variational analysis and the convergence of the finite element approximation of an electro-elastic contact problem with adhesion. *Arab Journal of Science and Engineering*. 2011; 36: 1501-1515.
- [16] Yuzhu Li, Qinghua Zhou. A non-monotone wolf-type line search strategy for unconstrained optimization. *Scholars Bulletin*. 2016; 216 (2): 581-587.
- [17] Bernard MAURIN. Recherche de forme et conception des structures innovantes. Mémoire d'habilitation à diriger des recherches de Montpellier II, France. 2007; 97.
- [18] Cyril DOUTHE. Etude des structures élancées précontraint en matériaux composites: application à la conception des gridshells. Thèse de doctorat à l'école nationale des ponts et chaussées, France. 2007; 275.
- [19] NGUYEN Anh Dung. Etude du comportement mécanique et du pliage d'un anneau de tensegrité à base pentagonale. Thèse de doctorat, université de Montpellier II, France. 2009; 140.
- [20] Khellaf Nadia. Comportement Non Linéaire Géométrique et Matériel Des Anneaux De Tensegrité Relâchement et Plastification Des Câbles. Thèse de doctorat Université Mohamed Khider – Biskra, Algérie. 2014; 154.
- [21] Ever Coarita, Leonardo Flores. Nonlinear analysis of structures cable-truss. *IACSIT, International Journal of Engineering and Technology*. June 2015; 7(3).
- [22] Guest SD. The Stiffness of Tensegrity Structures department of Engineering. University of Cambridge, Trumpington Street, Cambridge CB2 1PZ, UK. 2010.
- [23] Jérôme Quirant. Systèmes de tensegrité et autocontrainte: qualification, sensibilité et incidence sur le comportement. Thèse de doctorat université de Montpellier II, France. 2010; 195.
- [24] Sonia Lebofsky. Numerically Generated Tangent Stiffness Matrices for Geometrically Non-Linear Structures. Mémoire de Master Université de Washington, Etats-Unis. 2013; 77.
- [25] CJ Earls. Nonlinear Finite Element Analysis: Structures. School of Civil and Environmental Engineering, 220 Hollister Hall, Ithaca, NY 14853. September 15, 2016; 128.
- [26] Zhang JY, M Ohsaki. Optimization methods for force and shape Design of Tensegrity structures. 7th World Congress of Structural and Multidisciplinary Optimization. COEX Seoul. 21-25 may 2007; 40-49.
- [27] European Committee for Standardization. Eurocode 3: Design of steel structures - Part 1-1: General rules and rules for buildings. 2005.
- [28] Nagase K, RE Skeleton. Minimal mass tensegrity structures. *Journal of the International Association for Shell and Spatial Structures*. 2014; 55(1), 37-48.
- [29] Carpentieri G, RE Skelton, F Fraternali. Parametric Design of Minimal Mass Tensegrity Bridges Under Yielding and Buckling Constraints. Internal Report 2014-1: University of California, San Diego. 2014; 56.
- [30] Rhode-Barbargos L, N Bel Hadj Ali, R Motro, I.F.C. Smith. Designing tensegrity modulus for pedestrian bridges. *Engineering Structures*. 2010; 32 (4): 1158-1157.
- [31] Ada Amendolaa, Anastasiia Krushynska, Chiara Daraioc, Nicola M Pugno, Fernando Fraternali. Tuning frequency band gaps of tensegrity mass-spring chains with local and global prestress. *International journal of solids and structures*. 15 december 2018; 155: 47-56.
- [32] Keliu Tomas Zegard, Phanisri P Pratapa, Glaucio H Paulino. Unraveling tensegrity tessellations for metamaterials with tunable stiffness and bandgaps. *Journal of the mechanics and physics of solids*. october 2019; 131: 147-166.
- [33] Yoshihiro Kanno. Topology Optimization of Tensegrity Structures under self-weight loads. *Journal of the Operations Research Society of Japan*. The Operations Research Society of Japan. June 2012; 55(2): 125-145.
- [34] Rohith S, R Ramasubramani. Development and analysis of a pentagonal prism tensegrity system in roof structure. *International Journal of Civil Engineering and Technology*. may 2017; 8(5): 60-66.
- [35] OmarAloui, David Orden, Landolf Rhode-Barbarigos. Generation of planar tensegrity structures through cellular multiplication. *Applied Mathematical Modelling*, December 2018; 64: 71-92.
- [36] Mariano Modano, Ida Mascolo, Fernando Fraternali, Bigniew Bieniek. Numerical and Analytical Approaches to the Self-equilibrium Problem of Class $\theta = 1$ Tensegrity Metamaterials. *Frontier in Materials*, 21 february 2018.
- [37] Mvogo JK, LM Ayina Ohandja, L Seba Minsili, P Castera. Mechanical grading of structural timber and species conservation in the forest of the Congo Basin. *African Journal of Environmental Science and Technology*. February 2011; 5(2): 111-125.

- [38] Ron Dennis IT. Transport Ltd. Footbridges: A manual for Construction at Community and District Level. Rural Accessibility Technical Paper (RAPT) Series No.11. Geneva, International Labor Office. 2004; 185.
-

Author's short biography



Lezin Seba Minsili

A senior civil-structural engineer with a broad experience in design, construction, maintenance of civil structures, research and training in related multidisciplinary areas in Africa and Asia. He is graduated from the Transport University in Saint Petersburg-Russia, holds a Master and Ph.D. degrees from China, and occupied several administrative, engineering, teaching and research positions in Universities and Industries in China and Cameroon.



Kankeu Mbefoyo King Jackson

Kankeu Mbefoyo King Jackson is a Cameroonian Engineer, Master Degree in Civil Engineering and a Ph.D. Student, Department of Civil Engineering, Yaoundé National Advanced School of Engineering ENSPY, The University of Yaoundé 1. He works actually on Structural Engineering



Okpwe Mbarga Richard Placide

OKPWE MBARGA Richard Placide is a Civil Engineer trained at Ecole Hassania des Travaux Publics (Morocco) and specialized in transportation infrastructures with a Master of Sciences of Ecole Polytechnique de Paris (France). Since 2015 he is a Lecturer at ENSPY of the University of Yaoundé 1 (Cameroon) and is completing his PhD in BIM (Building Information Modeling).



Baleng Bleriot Landry

A graduate Engineer in structural Engineering holding key positions in design and construction engineering at MBA ENGINEERING AND SERVICES firm in Yaoundé-Cameroon. He is now pursuing a Master degree in structural Engineering in the LECM of ENSPY, The University of Yaoundé 1.